water

MDPI

Article

Greenhouse Crop Residue and Its Derived Biochar: Potential as Adsorbent of Cobalt from Aqueous Solutions

Irene Iáñez-Rodríguez, Mónica Calero *, Gabriel Blázquez and María Ángeles Martín-Lara *

Chemical Engineering Department, Faculty of Sciences, Avda, Fuentenueva s/n 18071 Granada, Spain; ireneir@ugr.es (I.I.-R.); gblazque@ugr.es (G.B.)

* Correspondence: mcaleroh@ugr.es (M.C.); marianml@ugr.es (M.Á.M.-L.); Tel.: +34-9-5824-3315 (M.C.); +34-9-5824-0445 (M.Á.M.-L.)

Received: 6 April 2020; Accepted: 29 April 2020; Published: 30 April 2020

Abstract: This work is focused on the removal of cobalt from aqueous solutions using the greenhouse crop residue and biochars resulting from its pyrolysis at different temperatures, which have not been previously used for this purpose. This study aims to provide insights into the effect of pyrolysis temperature as a key parameter on the cobalt adsorption capacity of these materials. Firstly, the main physicochemical properties of greenhouse crop residue and its biochars prepared under different pyrolysis temperatures were characterized by elemental analysis and FT-IR, among others. Then, the cobalt adsorption capacity of materials was evaluated in batch systems. The best results were obtained for the biochar prepared by pyrolysis at 450 °C (adsorption capacity of 28 mg/g). Generally, the adsorption capacity of the materials increased with pyrolysis temperature. However, when the treatment temperature was increased up to 550 °C, a biochar with worse properties and behavior than cobalt adsorbent was produced. Rather than surface area and other physical properties, functional groups were found to influence cobalt adsorption onto the prepared materials. The adsorption kinetics showed that the adsorption followed pseudo-second-order kinetics model. The obtained equilibrium data were fitted better by the Langmuir model rather than the Freundlich model. Finally, decomposition of loaded-materials was analyzed to assess their possible recycling as fuel materials. The study suggested that greenhouse crop residue can be used as a low-cost alternative adsorbent for cobalt removal from aqueous solutions.

Keywords: biochar; cobalt; heavy metals; pyrolysis; waste management; wastewater

1. Introduction

Industrial development has led to a massive generation of different kind of wastes. Concretely, the intensive agriculture, which consists of the culture of vegetables in greenhouses, has led to the generation of huge amounts of residual biomass (greenhouse crop residue, GCR). Little research has been carried out concerning this kind of waste. Greenhouses are productive systems characterized by an intensive and effective use of primary resources. This waste is very abundant worldwide and is currently used for compost production. This raw material has been studied and fully described in previous works carried out in our group [1,2]. The search for alternative uses for these materials is essential since it has both economic and environmental benefits.

On the other hand, another problem derived from some industrial activities is the pollution of water resources, which is a major problem worldwide. Industries such as jewelry, chemical, metallurgical, mining, tannery, electrical and electronics deliver heavy metals into the water, which are considered very toxic pollutants, even at very low concentrations due to their nonbiodegradability [3]. Some of

these elements are lead, cadmium, zinc, nickel, copper, mercury, chromium, cobalt and iron, which have shown to cause health and environmental problems [4]. The elimination of heavy metals can be carried out with a wide range of traditional technologies such as chemical precipitation, membrane filtration, oxidation, ozonation, ion-exchange and electrodialysis [5]. One of the most promising technologies is the biosorption—or bio-adsorption—which consists of the passive retention of the heavy metals in a biomass material. It has the advantage of being an efficient, low cost and ecofriendly technique. Additionally it gives a second use for a residual material [6]. A wide range of different materials such as sawdust [7], coffee husk [8], pinecone shells [9] and olive stones [10] among others have been proved as heavy metal biosorbents.

Recent studies have demonstrated the possibility of using different biomass waste as a precursor in the preparation of biomass carbon material. For example, Pellera et al. [11] focused on Cu(II) bio-adsorption by materials prepared at two different pyrolysis temperatures (300 °C and 600 °C). Wang et al. [12] evaluated the conversion of industrial cork waste to biochar by slow pyrolysis; Martín-Lara et al. [13] evaluated the lead adsorption capacity of carbonaceous materials obtained by slow pyrolysis of olive cake; Gai et al. [14] analyzed the effects of feedstock and pyrolysis temperature on ammonium and nitrate adsorption by biochar. Moreover, Liu et al. [15] investigated the bio-adsorption capacity of corn stalks biochars for removing Pb(II) from water. They determined that the best pyrolysis temperature for maximizing lead retention. These studies show the large potential of converting biomass waste into carbon materials as an adsorbent by pyrolysis.

Apart from the thermal treatments, other researchers have demonstrated that the adsorption capacity of the material can be enhanced by different chemical treatments with reactants such as citric acid and sodium hydroxide [16–18].

Batch experiments are necessary to evaluate fundamental information of the bio-adsorption process, such as adsorbent efficiency, optimum experimental conditions, adsorption rate and possibility of biomass regeneration [19]. In this work, the use of the greenhouse residue and its derived biochars prepared by pyrolysis at different temperatures as adsorbents for the removal of cobalt from aqueous solutions was proposed. Furthermore, some chemical treatments were tested with the GCR material in order to enhance its metal retention capacity. The main novelty is the use of the greenhouse crop residue for metal retention, which have never been studied before to the best of our knowledge.

2. Materials and Methods

2.1. Materials

The raw material used in this study was the greenhouse crop residue (GCR). It was collected from a treatment plant of vegetable wastes located in Motril (Spain). The residue was provided in October 2016 when the predominant crop residue biomass produced by the greenhouse agriculture was that derived from cultivation of *Capsicum annuum* L. (green pepper). Biomass sample was ground with an analytical mill (IKA MF-10) and it was sieved in a high vibratory sieve (CISA). The fraction between 0.250 and 1 mm was selected.

Biochar samples were prepared in a tubular muffle furnace Nabertherm model R50/250/12. Four pyrolysis temperatures were tested: 250 °C, 350 °C, 450 °C and 550 °C using an inert atmosphere of nitrogen with a flow of 100 L/h and a residence time of 15 min. An approximate mass of 10 g was weighed in the preparation of each sample. The samples were introduced in the oven once the set temperature was stable. The samples remained in the oven for the fixed residence time and then, the samples were removed from the furnace and kept in a desiccator until the temperature lowered. Finally, the solid left after the process was weighed and stored.

2.2. Characterization of the Materials

Different characterization methods were used to examine the effects of temperature of pyrolysis on the properties of the materials. All the measurements in this study were performed in duplicate to

ensure the quality and repeatability of the work. Average values and standard deviations are presented in the tables of the manuscript.

- Elemental analysis

The determination of the percentage of C, H, N, S and O was carried out by an elemental analyzer Fison's Instruments EA 1108 CHNS. Oxygen content was determined indirectly by difference, considering the content of ashes present in each of the samples [20].

- Proximate analysis

The quantification of moisture, volatile matter, fixed carbon and ash contents by standards methods was carried out. Ash content was determined according to standard ISO 18122:2015. Moisture content was determined by drying in an oven following the method described in the standard ISO 18134-3:2015. Volatile matter content was determined as the loss in mass (minus that due to moisture) when solid is subject to partial pyrolysis under standardized conditions following the procedure described in standard ISO 18123:2015. Finally, fixed carbon percentage was obtained by difference with moisture, ash and volatile matter percentages.

- Point of zero charge (PZC)

The point of zero charge was determined using the pH drift method, by adjusting pH of 100 mL of Milli-Q water with the materials to a value between 2 and 11, using 0.1 M hydrochloric acid and sodium hydroxide solutions.

- Fourier Transform Infrared Spectroscopy

Samples were analyzed in a FT-IR Spectrometer (Perkin-Elmer, Waltham, MA, USA, Spectrum, Stamford, CT, USA 65) in the range of 4000–400 cm^{-1}. This method enables the identification of pure inorganic and organic compounds. However, it is not a quantitative analysis [21].

- Surface analysis

The specific surface area was determined by the Brunner–Emmet–Teller (BET) method [22], while porosity was analyzed by porosimetry based on the calculation of adsorption–desorption isotherms with nitrogen and argon, using an ASAP 2420 equipment.

2.3. Cobalt Adsorption Experiments in Batch Systems

Adsorption experiments were performed with cobalt solutions to study the relationship between the solid phase concentration of cobalt (the amount of cobalt adsorbed per mass unit of solid material) and the cobalt solution phase concentration. The adsorption experiments were carried out with different initial cobalt concentrations (50, 100, 200, 400 and 800 mg/L). The stock solutions were prepared using $Co(NO_3)_2{\cdot}6H_2O$ salt and distilled water. Different samples were taken in each experiment: one before starting the experiment, others at different contact times and another one after two hours under stirring. The temperature was approximately 25 °C. A dose of 5 g/L of solid was used in each experiment. The adsorbent materials used were GCR and the biochars obtained after pyrolysis at 250 °C, 350 °C, 450 °C and 550 °C. The pH was kept in the range between 5 and 6 in all cases (natural pH of the cobalt solution), and always lower than 6.5 to avoid precipitation of cobalt as cobalt hydroxide.

The metal concentration was measured using an atomic adsorption spectrometer (Perkin-Elmer, Waltham, MA, USA, model AAnalyst 200). The removal capacity, in mg/g, was calculated using the Equation (1):

$$q_e = \frac{(c_i - c_f) \times V}{m} \quad (1)$$

where q_e is the removal capacity in mg/g, C_i and C_f represents the initial and the final metal concentration in mg/L, respectively. V is the volume of the solution in L and m is the mass of the adsorbent in g.

- Kinetics study

First, the study of adsorption kinetics was performed only for the native GCR material. A series of experiments were carried out at different concentrations and sample was taken in each test at different times in the interval between 0 and 120 min. Particular attention was paid in the first few minutes of the trial, as it is the time when the most change is observed in the concentration values. Table 1 reports the operating conditions for the various experiments carried out.

Table 1. Experimental conditions used for the study of the adsorption kinetics.

Test Number	1	2	3	4
Concentration, mg/L	25	50	100	200
Contact time, min	0, 5, 10, 15, 30, 60, 90, 120			
pH	<6–6.5			
Adsorbent dose, g/L	5			
Temperature, °C	25			
Volume, mL	150			

Then, tests were then carried out to analyze the adsorption kinetics of the biochar materials, setting an initial cobalt concentration of 25 mg/L and maintaining the remaining conditions equal to those indicated in Table 1.

- Equilibrium study

The experiments were conducted at different concentrations (50, 100, 200, 400 and 800 mg/L). Two samples were taken in each experiment: one initial sample before each experiment and another after two hours of shaking. The materials studied in this case were native GCR and biochar materials obtained by pyrolysis at different temperatures (250 °C, 350 °C, 450 °C, 550 °C). Table 2 summarizes the operating conditions used for each of the five materials studied.

Table 2. Experimental conditions used for the study of the adsorption equilibrium.

Test Number	1	2	3	4	5	6
Concentration, mg/L	50	100	200	400	800	1200
Contact time, min	0, 120					
pH	<6–6.5					
Adsorbent dose, g/L	5					
Temperature, °C	25					
Volume, mL	150					

2.4. Chemical Activation of the Material

To increase the adsorption capacity of GCR, different types of chemical treatment were tested for material activation. The different methods carried out were based on the work carried out by Romero-Cano et al. [23] and Feng et al. [16]. The methodology followed for the preparation of each of the materials is described below:

- Material 1 (M1)

A treatment with citric acid was carried out, followed by a wash with distilled water and a heat treatment at 120 °C. First, a citric acid solution (25 g of citric acid in 150 mL of water) was prepared. Once prepared, 12.5 g of GCR were submerged in this solution and kept under agitation for 90 min. The GCR was then recovered by filtration and washed with abundant distilled water. Finally, it was introduced for 3 h in an oven at 120 °C in an inert atmosphere.

- Material 2 (M2)

The procedure followed was the same as in the case of material M1, although the order of the steps was altered. In this case, first of all, the washing with citrus was carried out, followed by the heat treatment and finally the washing with distilled water.

- Material 3 (M3)

The procedure in this case consisted of a treatment with NaOH followed by a wash with distilled water. First, a 0.1 M solution of NaOH was prepared and 20 g of GCR was introduced in 200 mL of the dissolution. It was kept under agitation for 60 min.

- Material 4 (M4)

In this case, a basic treatment (NaOH) was combined with one acid (citric) and a wash. In this case, NaOH treatment was carried out as described for material M3. Subsequently, a treatment with citric acid was carried out 0.6 M for 2 h. Finally, the material was washed with distilled water.

- Material 5 (M5)

This material was prepared by treating the GCR with citric acid according to the procedure described for the material M1 but without any thermal treatment. Then the material was washed with distilled water.

2.5. Thermal Decomposition of the Loaded-Materials

The study of the influence on the thermal decomposition of the material due to adsorption of cobalt in its surface was carried out by thermogravimetry in an inert atmosphere of nitrogen. All experiments were conducted on a Perkin-Elmer thermobalance model STA 6000. In each experiment, an approximate amount of 25 mg sample, a heating rate of 20 °C/min and a nitrogen flow of 1.2 L/h were used.

3. Results and Discussion

3.1. Characterization of the Materials

3.1.1. Elemental and Proximate Analysis and Zero Point of Charge

Table 3 summarizes the results of elemental and proximate analysis and zero point of charge. The elemental analysis showed that all the materials contained negligible quantities of nitrogen and sulfur. Hydrogen content decreased as the pyrolysis temperature increased, due to the loss of volatile materials that occurs with heating. Carbon, meanwhile, decreased when pyrolysis treatment occurred at higher temperatures (450 °C and 550 °C). This decrease in the carbon percentage was not expected, as pyrolysis must generate a concentration of the carbon content in the samples (in the absence of oxygen in heating, carbon does not have to disappear in the process of pyrolysis). The decrease in carbon content may be due to the loss of carbon being lost with volatile materials during heating, and also because during the process of handling and extracting the sample from the furnace, contact with some oxygen can cause partial calcination. In general, the increase of the pyrolysis temperature would result in the increase of carbon content at the expense of hydrogen and oxygen content [24]. As for the oxygen content, since it is obtained by difference also taking into account the ash content of the sample, its value depends on the other parameters. Moreover, at 250 °C, the elemental analysis did not change much, suggesting that the pyrolysis did not proceed to a significant extent. With regard to the ratio of the C/H, it increased as the pyrolysis temperature increased, being especially significant the increase of the C/H ratio when the pyrolysis temperature was changed from 350 °C to 450 °C. The results of elemental analysis presented the same tendencies in similar studies carried out by other authors, except for the carbon, which showed to increase in other works because of the aforementioned reason [5].

Table 3. Elemental analysis, proximate analysis and point of zero charge of the samples.

Analysis		Greenhouse Crop Residue	250 °C	350 °C	450 °C	550 °C
Proximate Analysis	% Moisture	7.43 ± 0.37	1.89 ± 0.09	4.31 ± 0.19	4.33 ± 0.21	3.00 ± 0.12
	% Volatile matter (VM)	56.66 ± 2.80	52.31 ± 2.14	41.11 ± 2.06	21.43 ± 1.01	15.36 ± 0.56
	% Ashes	23.97 ± 1.09	30.31 ± 1.21	38.34 ± 1.45	52.35 ± 2.12	55.41 ± 1.87
	% Fixed carbon (FC)	11.95 ± 0.49	15.49 ± 0.70	16.23 ± 0.68	21.88 ± 0.87	26.24 ± 1.13
	VM/FC ratio	4.74	3.38	2.53	0.98	0.59
Elemental Analysis	% C	34.02 ± 1.70	35.29 ± 1.67	34.29 ± 1.41	28.84 ± 1.44	21.34 ± 1.01
	% H	5.89 ± 0.92	4.83 ± 0.24	4.59 ± 0.32	1.39 ± 0.07	0.77 ± 0.03
	% O	32.95 ± 1.56	28.08 ± 1.04	20.27 ± 1.10	16.22 ± 0.81	21.29 ± 1.60
	% S	0.02 ± 0.00	0.02 ± 0.00	0.02 ± 0.00	0.03 ± 0.01	0.05 ± 0.01
	% N	3.15 ± 0.16	1.47 ± 0.07	2.39 ± 0.21	1.17 ± 0.60	1.14 ± 0.08
	C/H ratio	5.78	7.31	7.47	20.75	27.71
Point of Zero Charge (PZC)		6.30 ± 0.25	6.28 ± 0.14	7.22 ± 0.30	7.77 ± 0.22	9.23 ± 0.18

In regard to proximate analysis, the results showed that moisture content was reduced after the pyrolysis process and it seemed to be not very dependent on the pyrolysis temperature. The moisture present in the samples corresponded to the equilibrium moisture. The depletion in the moisture could be due to the increase of the hydrophobicity of the materials after the pyrolysis due to the degradation of the sites which retain the water in the material. The destruction of those sites occurs at low temperature (more or less 200 °C), and for that reason the moisture content did not strongly depend on the pyrolysis temperature. Concerning to the volatile matter, it significantly decreased as the treatment temperature increased, which is logical as the compounds which were mainly eliminated during pyrolysis at those temperatures were volatiles. Fixed carbon showed an increase as the pyrolysis temperature increased, although this increase is milder at higher temperatures, which would be related to what is indicated by the decrease in carbon found in the elemental analysis. A little quantity of oxygen could have entered in the container when it was removed from the muffle, causing a diminishing in the fixed carbon content in the sample. With regard to ash content, it considerably increased with increase in pyrolysis temperature. This is because the ashes are composed of inorganic elements that remain after heating in the generated biochar and, therefore, their content is concentrated by the volatilization of the other elements such as C, H, N and O. The results were very similar to those found by other authors for pyrolysis of avocado seed [25], bone [26], poplar [24] or rice husk [27]. Finally, some authors have reported that for a biochar to be stable, the ratio between its volatile matter content (VM) and its fixed carbon content (FC) must be lower than 1. In addition, the biochar is more stable if the ratio approaches zero [28]. From the VM/FC ratio calculated for the materials studied in this work, biochars obtained by pyrolysis at 450 °C and 550 °C showed a stable structure, increasing with the increase in temperature.

Finally, PZC was increased from acidic values (6.30 and 6.28 for native and sample obtained from pyrolysis at 250 °C) to a basic value of 9.23 for the material derived from pyrolysis at 550 °C. At a pH solution value higher than the PZC, the surface of the materials is negatively charged; in contrast, the surface turns positive at a pH solution value below PZC. In the adsorption tests, the pH was kept in the range between 5 and 6. Therefore, during the adsorption tests all the samples carried a net positive charge. Thus, the adsorption of cobalt cations on solid diminishes due to electrostatic attraction, probably more for material pyrolyzed at 550 °C.

3.1.2. FTIR

Furthermore, infrared spectroscopy was carried out in order to investigate the changes in the material structure caused by the pyrolysis process, as shown in Figure 1.

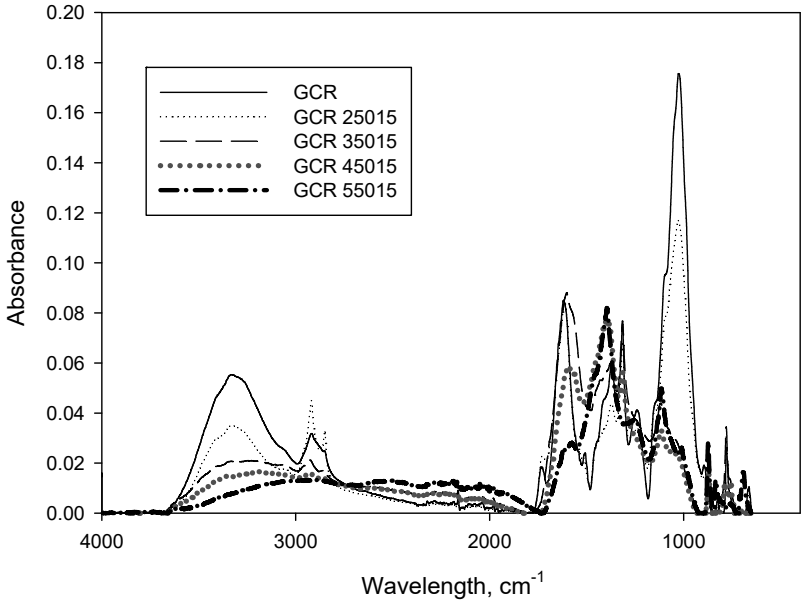

Figure 1. Infrared spectrum of the greenhouse crop residue (GCR) and biochars resulting from pyrolysis of GCR at different temperatures (250 °C, 350 °C, 450 °C and 550 °C).

In general terms, the absorbance decreased as the pyrolysis temperature increased, compared to the raw material. The higher the treatment temperature was, the greatest changes were observed. The identification of each peak for GCR sample was carried out in a previous study [2]. In this paper, the changes observed due to thermal treatment at high temperatures were analyzed. The peak at 3330 cm^{-1} corresponded to –OH stretching. It was lowered considerably for temperature higher than 350 °C indicating the elimination of this kind of bonding. This is in accordance with the decrease in O and H content observed in elemental analysis. At those temperatures the elimination of water and the degradation of cellulose and hemicellulose occurred, decreasing the –OH peak. On the other hand, the peaks observed between 2750 and 2980 cm^{-1} represented CH-stretching was not observed at temperatures above 450 °C. The peak around 1730 cm^{-1} corresponded to C=O stretching. It was totally eliminated at high temperatures, indicating the elimination of aldehyde, ketone and acid organic components from the samples. The peak observed at 1620 cm^{-1} which represented the aromatic skeletal vibration of lignin. It was also lowered but only at the highest temperatures (450 °C and 550 °C). For that reason, it could be affirmed that the pyrolysis affected the lignin at those temperatures. The peaks between 1509 and 1200 cm^{-1} corresponded to functional groups present in lignin. They were the less affected after the pyrolysis treatment. It could be because among all the main components of biomass materials (cellulose, hemicellulose and lignin), lignin was the most resistant fraction. High peaks were observed for the raw GCR in the range of 1000 and 1200 cm^{-1} for raw biomass sample. Those peaks were strongly lowered with thermal treatment, indicating that cellulose and hemicellulose groups were broken due to depolymerization reactions. The most affected fraction by the thermal treatment was hemicellulose, followed by cellulose. The lignin was the most thermal resistant fraction, although at high temperatures it started its degradation.

3.1.3. BET Surface, Pore Size and Volume

Table 4 shows the surface properties of the materials including BET surface area, average pore diameter and total pore volume. The BET surface area ranged from 6.2 to 9.2 m^2/g. These values are low when compared to commercial adsorbents such as activated carbon. The biochar exhibited very low surface area compared to those reported in the literature [29,30]. This suggests that cobalt adsorption was possibly carried out by ion exchange and complexation on the surface of the material more so than physical adsorption. Low porosity also indicates that the process control mechanism

was not diffusion [31]. If different samples are compared, the surface area showed a higher value for the biochar obtained at 450 °C. In general, an increase in pyrolysis temperature until 450 °C resulted in an increase in surface area, pore size and pore volume. These changes were attributed to the degradation of the lignocellulosic structure, devolatilization of biomass components and opening cracks in the material [15,26,32]. However, a further increase of temperature until 550 °C resulted in a decrease of the surface area (7.5 m^2/g), probably due to shrinkage and realignment in the char structure. Similar results were also reported by other researchers as Alkurdi et al. [26], Angin and Sensoz [32], Ji et al. [30], Liu et al. [15], Patel et al. [33] and Zhang et al. [34]. For example, Ji et al. [30] studied the adsorption of methylene blue onto novel biochars prepared from Magnolia grandiflora leaves and reported that when the pyrolysis temperature rose from 500°C to 550°C, the BET surface area decreased. On the contrary, the pore diameter increased. These authors indicated that this might be for the collapse of the pore wall caused by high temperature; thus, some small mesoporous become large mesoporous.

Table 4. Brunner–Emmet–Teller (BET) surface area, average pore diameter and total pore volume of the samples.

Material	BET Surface Area, m^2/g	Average Pore Diameter, Å	Total Pore Volume, cm^3/g
GCR	6.2 ± 0.31	47.5 ± 2.83	0.0073 ± 0.0004
GCR 250-15	7.3 ± 0.73	45.6 ± 2.28	0.0116 ± 0.0005
GCR 350-15	9.1 ± 0.41	57.1 ± 2.68	0.0105 ± 0.0006
GCR 450-15	9.2 ± 0.64	62.7 ± 3.41	0.0142 ± 0.0010
GCR 550-15	7.5 ± 0.93	73.2 ± 3.36	0.0138 ± 0.0013

3.2. Cobalt Adsorption by GCR and Biochars Resulting from Its Pyrolysis

3.2.1. Effect of Contact Time and Adsorption Kinetics

Studying the effect of contact time to achieve equilibrium and analyzing the kinetics of cobalt adsorption onto GCR and its biochars is crucial to be able to determine the nature of the adsorption process. This study allows knowing the rate at which cobalt is removed from the aqueous medium and serves to select the most favorable conditions for the treatment of effluents [35,36].

Firstly, trials were conducted with the native material at different initial concentrations of cobalt, as shown in Figure 2. For the native GCR, the adsorption process was fast, since for all the concentrations studied, equilibrium was reached before 30 min of operating time. Two important stages could be observed. The first one was before the 5 min of operation, when the 50% or more of the total cobalt was adsorbed on the solid surface for all tested initial cobalt concentrations. The second one occurred after 5 min of operation. It showed that cobalt removal rate increased gradually until reach the equilibrium. It should be highlighted that the equilibrium was reached faster for the lowest initial cobalt concentration. In contrast, the amount of cobalt adsorbed onto GCR was higher when the initial concentration was higher, reaching values of around 14 mg/g for an initial concentration of 200 mg/L. These results indicated that increasing the initial cobalt concentration promoted the interaction between the cobalt ions and the material surface, and provided a significant driving force for mass transfer between the adsorbate and the adsorbent which is advantageous for adsorption [12,37].

The adsorption kinetics of the different materials (native GCR and its biochars derived from pyrolysis at different temperatures) was then analyzed, choosing an initial cobalt concentration of 25 mg/L, as shown in Figure 3. Similar trends were observed in all of them: they all reached the equilibrium around 30 min and the fastest adsorption phase occurred in the first 5 min of operation. In addition, the results clearly show that pyrolysis at the temperature of 250 °C did not affect the adsorption capacity of the material. The highest adsorption capacity was obtained for temperatures of 350 °C and 450 °C at an initial cobalt concentration of 25 mg/L. Both temperatures offered very similar results, reaching a value close to 4 mg/g. On the other hand, it is observed that the temperature

of 550 °C produced a decrease in adsorption capacity, although it is still higher than that of untreated GCR. Therefore, it could be concluded that the pyrolysis temperatures that most favored the adsorbent capacity of the GCR are 350 °C and 450 °C. The pyrolysis temperature 550 °C would constitute an unnecessary energy expenditure that also does not maximize the adsorption capacity of the material. These results could be related to the characterization results obtained for this material, for example, it had a specific surface area lower than biochars obtained at a temperature of 350 °C or 450 °C, and a very high PZC.

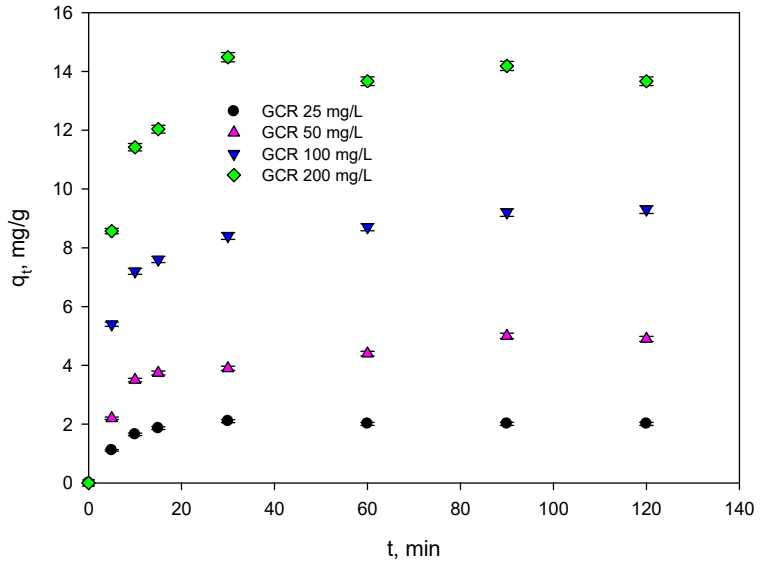

Figure 2. Kinetic curves of cobalt adsorption onto GCR at different initial cobalt concentrations (25, 50, 100 and 200 mg/L).

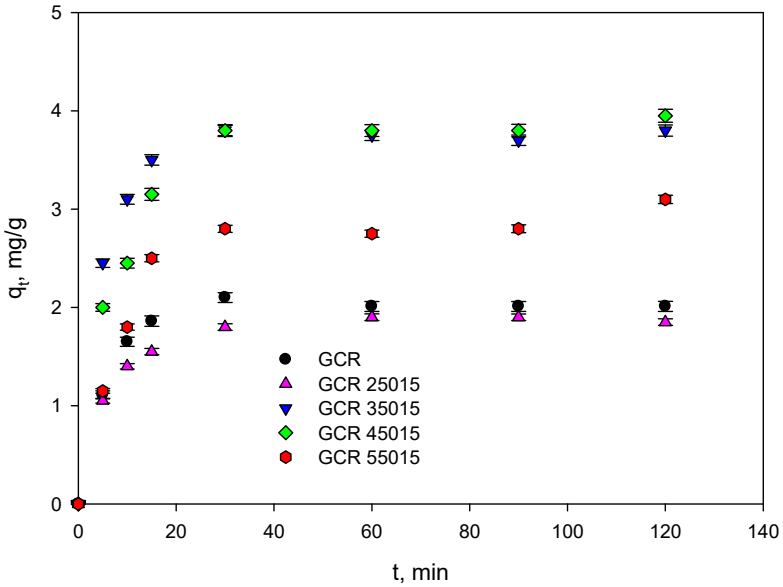

Figure 3. Kinetic curves of cobalt adsorption onto GCR and biochars resulting from pyrolysis of GCR at different temperatures (250 °C, 350 °C, 450 °C and 550 °C) and an initial Co concentration of 25 mg/L.

Experimental data were fitted to the kinetic models of pseudo-first order [38] and pseudo-second order [39]. These kinetic models are summarized in the Equations (2) and (3):

$$q_t = q_e \times \left(1 - e^{-k_1 \times t}\right) \quad (2)$$

$$q_t = \frac{t}{\frac{1}{k_2 \times {q_e}^2} + \frac{t}{q_e}} \quad (3)$$

where q_e and q_t are the amount of cobalt adsorbed (mg/g) at equilibrium and at time t (min), respectively; k_1 (min^{-1}) and k_2 ($g \cdot mg^{-1} \cdot min^{-1}$) are the pseudo-first and pseudo-second order rate constants, respectively.

Table 5 shows the parameters of both models. The pseudo-second order model fits the experimental results very well, with R^2 values close to the unit. Likewise, the calculated values of the equilibrium adsorption capacity (q_e) from pseudo-second order show good agreement with the experimental values meaning that chemical effect is involved in the adsorption of cobalt on the studied materials. This result indicates that chemical adsorption such as ions exchange or coordination is involved in cobalt adsorption process [40]. However, although the pseudo-first order model shows a worse adjustment of the results, the calculated q_e values are also very close to the experimental ones. With regard to the kinetic constant, in general, for both the pseudo-first order model and the pseudo-second order model, the kinetic constant decreases as the temperature of the pyrolysis process rises, indicating that while adsorption generally reaches higher adsorption capacities the process goes down more slowly until equilibrium is reached, although the changes are not relevant because it is not evident in Figure 3. These results are in accordance with those obtained by other authors in metal adsorption studies using residues or biochars derived from pyrolysis of residues [12].

Table 5. Kinetics parameters of the pseudo-first order and pseudo-second order models.

Material	Pseudo-First Order			Pseudo-Second Order		
	q_e	k_1	R^2	q_e	k_2	R^2
GCR	2.036	0.162	0.987	2.057	0.243	0.998
GCR 250-15	1.855	0.145	0.963	1.933	0.164	0.999
GCR 350-15	3.745	0.196	0.975	3.842	0.138	0.998
GCR 450-15	3.846	0.112	0.959	4.086	0.051	0.998
GCR 550-15	2.905	0.107	0.959	3.177	0.045	0.998

3.2.2. Effect of Initial Cobalt Concentration and Adsorption Isotherms

Cobalt adsorption isotherms were obtained, as shown in Figure 4. The adsorption isotherms were all type-I, characterized by a sharp increase at the initial stage (low cobalt concentrations) followed by a low-moderate progress at higher concentrations. The maximum adsorption capacity is similar for native material and biochars prepared at the lowest temperatures (250 °C and 350 °C). The highest uptake of cobalt was obtained for the biochar prepared by pyrolysis at 450 °C with a maximum adsorption capacity of approximately 28 mg/g. Also, the biochar prepared at 550 °C showed a good adsorption capacity close to 22 mg/g. Others researchers as Saletnik et al. [41] studying the adsorption of cadmium, lead and cobalt with a biochar obtained from cones of larch and spruce, obtained the best adsorption capacity for the treated material at 500 °C for 5 min, these being conditions very similar to the optimal conditions obtained between work (450 °C and 15 min).

Langmuir [42] and Freundlich [43] isotherm adsorption models were used to fit the experimental data of cobalt adsorption. These kinetic models are summarized in the Equations (4) and (5):

$$q_e = \frac{b\, q_m C_e}{1 + b\, C_e} \quad (4)$$

$$q_e = K_F C_e^{\frac{1}{n}} \quad (5)$$

where q_e (mg/g) is the equilibrium adsorption capacity of the adsorbent; q_m is the maximum adsorption capacity (mg/g); b (L/mg) is the constant of the affinity between the adsorbent and the adsorbate;

C_e (mg/L) is the equilibrium concentration after adsorption; K_F (mg/g)·(L/mg)$^{1/n}$ is the Freundlich constant related to the adsorption capacity and 1/n describes surface heterogeneity.

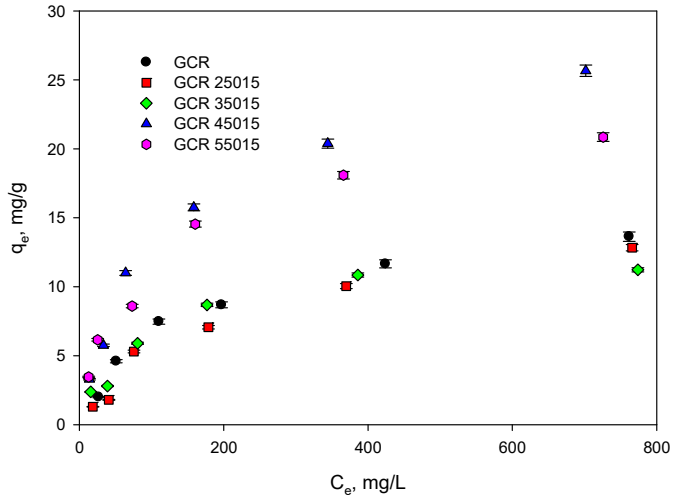

Figure 4. Isotherm curves of cobalt adsorption onto GCR and biochars resulting from pyrolysis of GCR at different temperatures (250 °C, 350 °C, 450 °C and 550 °C).

Table 6 shows the fitting parameters. The Langmuir model reproduced experimental data better than Freundlich model. In addition, the fit was better for biochars prepared at a higher temperature of pyrolysis. With regard to the results obtained with the Langmuir model, it is observed that the biochar prepared at 450 °C showed a higher cobalt adsorption capacity, with a q_m value close to 31 mg/g, much higher than the value obtained with the native material (13.58 mg/g). However, the loss of mass in pyrolysis is important when assessing the improvement of its adsorptive properties. If a great mass is lost during pyrolysis, it may not compensate the improvement of its properties as adsorbent. The mass loss during different pyrolysis treatments at different operating temperatures are also shown in Table 6. Significant impact of increasing pyrolysis temperature was observed on mass loss. The mass loss increased with increasing pyrolysis temperature from 8.96% at 250 °C to 59.08% at 550 °C. With increasing pyrolysis temperature, the thermal degradation of GCR into compounds of low molecular weight (released as volatiles including no condensable and condensable gases) occurred, leading to the increase the mass loss. A corrected adsorption capacity value was calculated taking into account this mass loss ($q_{m,cor}$). The adsorption capacity was still higher for the biochar obtained at an operating temperature of 450 °C, but the difference with native material was very low. With respect to the results shown by the fit to the Freundlich model, the values of n were lower than 1, indicating favorable adsorption of cobalt ions by studied materials under the selected experimental conditions [44].

Table 6. Parameters of the Langmuir and Freundlich isotherm models.

Material	Langmuir Model					Freundlich Model		
	q_m, mg/g	Loss of Mass, %	q_{mcor}, mg/g	b, L/mg	R^2	n	K_F, (mg/g)·(L/mg)$^{1/n}$	R^2
GCR	13.584	0.000	–	0.010	0.985	2.259	0.706	0.850
GCR 250-15	14.339	8.960	13.054	0.005	0.980	1.778	0.304	0.899
GCR 350-15	12.289	50.740	6.054	0.012	0.997	2.525	0.857	0.897
GCR 450-15	30.984	55.100	13.912	0.007	0.997	2.090	1.157	0.948
GCR 550-15	25.548	59.080	10.454	0.009	0.993	2.419	1.459	0.963

Finally, in order to compare the results with those obtained in previous studies by other researchers, Table 7 shows the values of the cobalt adsorption capacity obtained using different materials. The GCR has reasonable cobalt adsorption capacity, although it is lower than many other materials studied earlier.

Table 7. Adsorption capacities of different materials.

Material	q_m, mg/g	Reference
Treated carob shells	17.41	Farnane et al. [44]
Coir pith	12.82	Parab et al. [45]
Glebionis coronaria L.	24.52	Tounsadi et al. [46]
Diplotaxis harra	33.02	Tounsadi et al. [46]
Lemon peel	22.00	Bhatnagar et al. [47]
Seaweed	20.63	Vijayaraghavan et al. [48]
Hemp fibers	13.58	Tofan et al. [49]
Black carrots	5.35	Güzel et al. [50]
P. *Capillacea*	52.60	Ibrahim [51]
Rose waste biomass	13.90	Javeda et al. [52]
Sunflowers	11.68	Oguz and Ersoy [53]
Activated carbon prepared from hazelnut shells	11.57	Demirbas [54]
Greenhouse crop residue	13.58	This work

3.2.3. Chemical Activation of the GCR

In order to improve the adsorption capacity of the GCR through an alternative procedure, the effect of different types of chemical activation process was tested. The cobalt removal (%) and the adsorption capacity of the different materials (native and chemically activated) were calculated, using two initial cobalt concentrations, 25 and 100 mg/L, as shown in Figure 5.

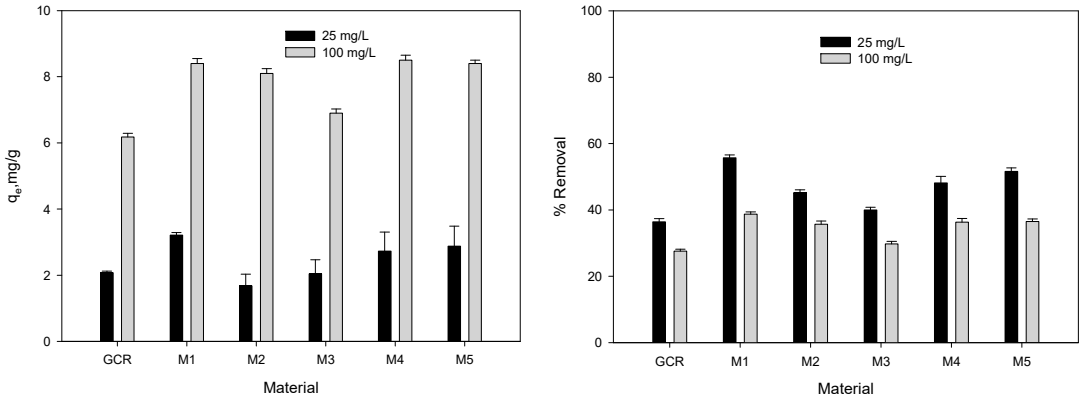

Figure 5. Adsorption capacity (left) and removal (%) (right) of cobalt adsorption onto GCR and materials resulting from chemical activation of GCR.

All chemical treatments provided an improvement in the adsorption capacity of the material and in the cobalt removal. The improvements were most noticeable for the initial concentration of 100 mg/L. The material that offers less satisfactory results was the M3. The rest of the treatments offer quite similar results. The M5 was chosen as the best treatment, since, apart from offering good results, the method of preparation of the material is the simplest and most economical and does not require temperature application.

Once the M5 material was chosen, the cobalt isotherm of the material was developed and compared to that of the native material, as shown in Figure 6. At low concentrations the adsorption capacity of both materials was very similar. However, when concentration increased, the differences were more evident. Additionally, it should be highlighted that the native material had practically already achieved

its maximum adsorption capacity at a concentration of around 400 mg/L. However, the M5 material showed a positive trend with an upward slope, which seems to indicate that the differences between the native material and the M5 will become even more noticeable at high concentrations. The data for the material processed M5 were adjusted to the Langmuir model to compare with the results obtained with the native material. The results showed a q_m value for M5 of 27.39 mg/g (R^2 = 0.998), much higher than that obtained for the native material (13.58 mg/g). However, again, the loss of mass that occurred during the treatment of the material should be considered, in order to obtain a corrected q_m value which could be more comparative. In this case the $q_{m,cor}$ value for the sample with the M5 treatment was 19.88 mg/g. This work is focused on making the cost of using this material the lowest possible. Although the value of $q_{m,cor}$ is still higher than that obtained with the native material, this increase in adsorption capacity does not justify the use of treatment for this material.

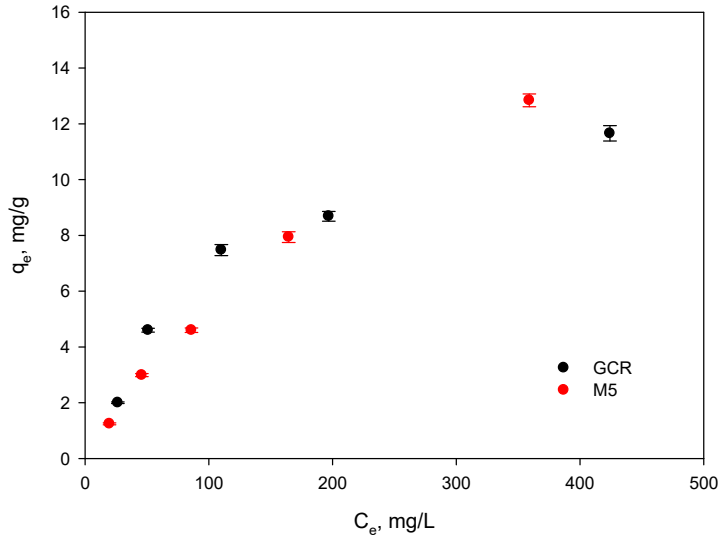

Figure 6. Isotherm curves of cobalt adsorption onto GCR and M5 material (obtained by chemical activation of GCR).

3.3. Thermal Decomposition of the Cobalt-Loaded GCR

During the adsorption process, cobalt is retained by the material. One of the possibilities of final disposal of cobalt-loaded materials is its use for power generation. Therefore, it is important to know the effect that metal impregnation has on the thermal decomposition of the material. The thermal decomposition of the GCR and biochars resulting from pyrolysis of GCR at different temperatures (250 °C, 350 °C, 450 °C and 550 °C) was performed, as shown in Figure 7. Differences were observed in the amount of residual solid after thermal decomposition of different materials. The material that left the most fraction of residual solid is the native GCR. On the other hand, the material that left fewer residual solid at the end of thermal decomposition was the washed GCR. With respect to the cobalt-loaded samples, its residue content was lower than that of the native material, which is justified by the adsorption process because similar thermogravimetric curves between cobalt-loaded and washed sample was observed. However, as the initial cobalt concentration used in adsorption was higher, the final solid fraction after the thermal decomposition process was higher. This suggested that the cobalt remained as part of the ashes. Furthermore, the decomposition of the native GCR occurs at a lower temperature indicating that cobalt could have a stabilizing effect, delaying the onset of thermal decomposition of the material. In addition, when the concentration of cobalt increased, the peak which appeared around 350 °C decreased its intensity in the derivative thermogravimetric curve (DTG), indicating a loss of mass at a lower rate in that temperature range. Finally, when cobalt concentrations were high, there was no decomposition at 750–800 °C, which means that perhaps cobalt prevents the volatilization of some inorganic compounds.

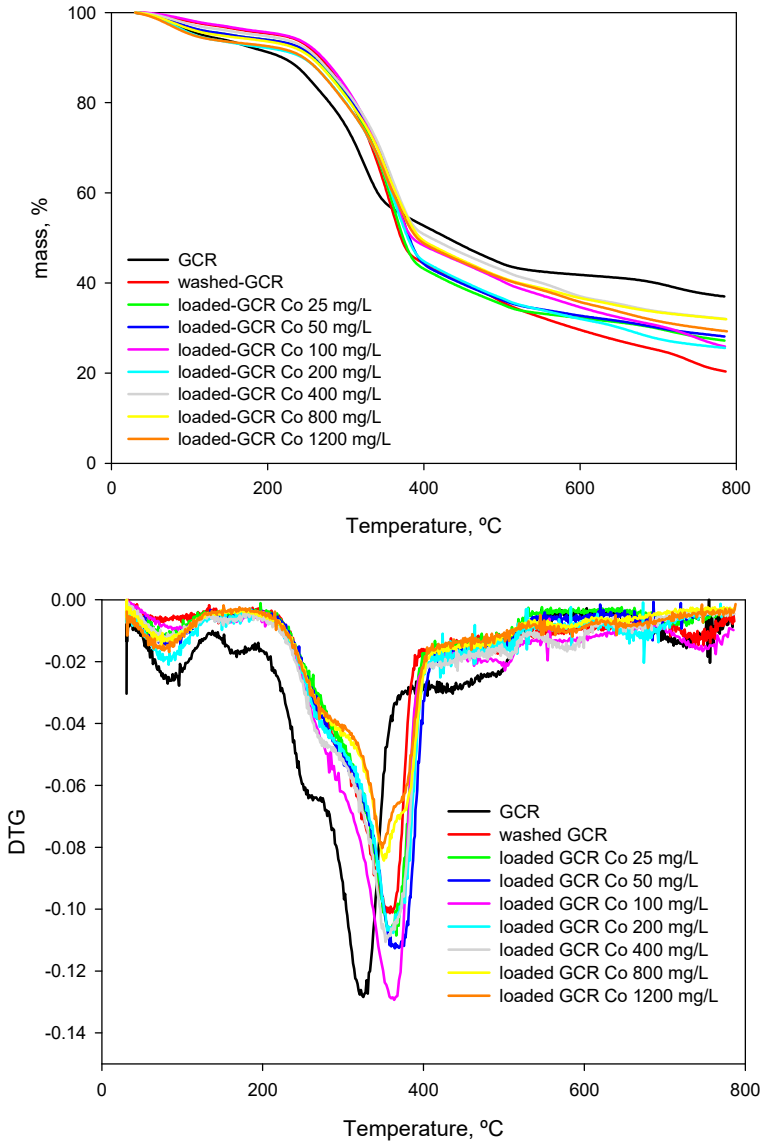

Figure 7. Thermogravimetric curves of the decomposition of GCR, washed GCR and cobalt-loaded GCR.

4. Conclusions

In this research, the GCR and biochars prepared by pyrolysis at different operating temperatures were analyzed for the cobalt removal from aqueous solutions. The characterization results indicated that modification resulted in the reduction of volatile matter and increase on carbon content. Also, a very little increment of the BET surface area, average pore diameter as well as total pore volume was observed. Both GCR and the prepared biochars showed good adsorption capacity for cobalt ions. The pseudo second-order kinetics model was suitable for describing the removal of cobalt by all the materials. The Langmuir model fitted very well the experimental isotherm data. The higher maximum adsorption capacity was obtained for biochar derived of pyrolysis of GCR at 450 °C reaching a value of 30.98 mg/g. Chemical treatments provided an improvement in the adsorption capacity of the material and in the cobalt removal. The improvements were most noticeable for the initial concentration of 100 mg/L. The M5 was chosen as the best treatment, since, apart from offering good results, the method of preparation of the material is the simplest and most economical and does not require temperature application. Finally, based on the study of thermal decomposition of materials, cobalt showed a stabilizing effect, delaying the onset and rate of thermal decomposition of the materials.

Cobalt also seems to remain as part of the ashes due to the increase in the final solid fraction kept after the thermal decomposition process when cobalt-loaded GCR was used.

Author Contributions: Conceptualization, M.C. and M.Á.M.-L.; methodology, I.I.-R. and M.C.; software, G.B.; formal analysis, I.I.-R., M.C. and M.Á.M.-L.; investigation, I.I.-R.; resources, M.C.; data curation, G.B.; writing—original draft preparation, I.I.-R. and M.Á.M.-L.; writing—review and editing, M.C. and M.Á.M.-L.; supervision, M.C. and M.Á.M.-L. All authors have read and agreed to the published version of the manuscript.

Funding: This research received no external funding.

Conflicts of Interest: The authors declare no conflict of interest.

References

1. Callejón-Ferre, Á.-J.; Martí, B.V.; López-Martínez, J.; Manzano-Agugliaro, F. Greenhouse crop residues: Energy potential and models for the prediction of their higher heating value. *Renew. Sustain. Energy Rev.* **2011**, *15*, 948–955. [CrossRef]
2. Iáñez-Rodríguez, I.; Martín-Lara, M.; Blázquez, G.; Pérez, A.; Calero, M. Effect of torrefaction conditions on greenhouse crop residue: Optimization of conditions to upgrade solid characteristics. *Bioresour. Technol.* **2017**, *244*, 741–749. [CrossRef]
3. Hossain, M.; Ngo, H.-H.; Guo, W.; Nguyen, T.V.; Vigneswaran, S. Performance of cabbage and cauliflower wastes for heavy metals removal. *Desalin. Water Treat.* **2013**, *52*, 844–860. [CrossRef]
4. Abdolali, A.; Ngo, H.-H.; Guo, W.; Zhou, J.L.; Zhang, J.; Liang, S.; Chang, S.W.; Nguyen, D.D.; Liu, Y. Application of a breakthrough biosorbent for removing heavy metals from synthetic and real wastewaters in a lab-scale continuous fixed-bed column. *Bioresour. Technol.* **2017**, *229*, 78–87. [CrossRef]
5. Rao, R.A.K.; Khatoon, A. Aluminate treated *Casuarina equisetifolia* leaves as potential adsorbent for sequestering Cu(II), Pb(II) and Ni(II) from aqueous solution. *J. Clean. Prod.* **2017**, *165*, 1280–1295. [CrossRef]
6. Martín-Lara, M.; Iáñez-Rodríguez, I.; Blázquez, G.; Quesada, L.; Pérez, A.; Calero, M. Kinetics of thermal decomposition of some biomasses in an inert environment. An investigation of the effect of lead loaded by biosorption. *Waste Manag.* **2017**, *70*, 101–113. [CrossRef] [PubMed]
7. Rafatullah, M.; Sulaiman, O.; Hashim, R.; Ahmad, A. Adsorption of copper (II), chromium (III), nickel (II) and lead (II) ions from aqueous solutions by meranti sawdust. *J. Hazard. Mater.* **2009**, *170*, 969–977. [CrossRef] [PubMed]
8. Oliveira, W.E.; Franca, A.S.; Oliveira, L.S.; Rocha, S.D. Untreated coffee husks as biosorbents for the removal of heavy metals from aqueous solutions. *J. Hazard. Mater.* **2008**, *152*, 1073–1081. [CrossRef] [PubMed]
9. Martín-Lara, M.; Blázquez, G.; Calero, M.; Almendros, A.; Ronda, A. Binary biosorption of copper and lead onto pine cone shell in batch reactors and in fixed bed columns. *Int. J. Miner. Process.* **2016**, *148*, 72–82. [CrossRef]
10. Godoy, V.; Iáñez-Rodríguez, I.; Pérez, A.; Martín-Lara, M.; Blázquez, G. Neural fuzzy modelization of copper removal from water by biosorption in fixed-bed columns using olive stone and pinion shell. *Bioresour. Technol.* **2018**, *252*, 100–109. [CrossRef]
11. Pellera, F.-M.; Giannis, A.; Kalderis, D.; Anastasiadou, K.; Stegmann, R.; Wang, J.-Y.; Gidarakos, E. Adsorption of Cu(II) ions from aqueous solutions on biochars prepared from agricultural by-products. *J. Environ. Manag.* **2012**, *96*, 35–42. [CrossRef] [PubMed]
12. Wang, Q.; Lai, Z.; Mu, J.; Chu, D.; Zang, X. Converting industrial waste cork to biochar as Cu (II) adsorbent via slow pyrolysis. *Waste Manag.* **2020**, *105*, 102–109. [CrossRef]
13. Martín-Lara, M.; Pérez, A.; Vico-Pérez, M.; Godoy, V.; Blázquez, G. The role of temperature on slow pyrolysis of olive cake for the production of solid fuels and adsorbents. *Process. Saf. Environ. Prot.* **2019**, *121*, 209–220. [CrossRef]
14. Gai, X.; Wang, H.; Liu, J.; Zhai, L.; Liu, S.; Ren, T.; Liu, H. Effects of Feedstock and Pyrolysis Temperature on Biochar Adsorption of Ammonium and Nitrate. *PLoS ONE* **2014**, *9*, 113888. [CrossRef] [PubMed]
15. Liu, J.; Huang, S.; Chen, K.; Wang, T.; Mei, M.; Li, J. Preparation of biochar from food waste digestate: Pyrolysis behavior and product properties. *Bioresour. Technol.* **2020**, *302*, 122841. [CrossRef]
16. Feng, D.; Bai, B.; Wang, H.; Suo, Y. Thermo-chemical modification to produce citric acid–yeast superabsorbent composites for ketoprofen delivery. *RSC Adv.* **2015**, *5*, 104756–104768. [CrossRef]

17. Romero-Cano, L.A.; García-Rosero, H.; Gonzalez-Gutierrez, L.; Baldenegro-Pérez, L.A.; Carrasco-Marín, F. Functionalized adsorbents prepared from fruit peels: Equilibrium, kinetic and thermodynamic studies for copper adsorption in aqueous solution. *J. Clean. Prod.* **2017**, *162*, 195–204. [CrossRef]
18. Romero-Cano, L.A.; Gonzalez-Gutierrez, L.; Baldenegro-Pérez, L.A.; Carrasco-Marín, F. Grapefruit peels as biosorbent: Characterization and use in batch and fixed bed column for Cu(II) uptake from wastewater. *J. Chem. Technol. Biotechnol.* **2017**, *92*, 1650–1658. [CrossRef]
19. Abdi, O.; Kazemi, M. A review study of biosorption of heavy metals and comparison between different biosorbents. *J. Mater. Environ. Sci.* **2015**, *6*, 1386–1399.
20. Fernández-González, R.; Martín-Lara, M.; Iáñez-Rodríguez, I.; Calero, M. Removal of heavy metals from acid mining effluents by hydrolyzed olive cake. *Bioresour. Technol.* **2018**, *268*, 169–175. [CrossRef]
21. Escobar Barrios, V.A.; Rangel Méndez, J.R.; Pérez Aguilar, N.V.; Andrade Espinosa, G.; Dávila Rodríguez, J.L. FTIR—An Essential Characterization Technique for Polymeric Materials. Infrared Spectroscopy—Materials Science, Engineering and Technology, 2012. Available online: http://www.intechopen.com/books/infrared-spectroscopy-materials-science-engineering-and-technology/ftir-an-essential-characterization-technique-for-polymeric-materials (accessed on 30 April 2020).
22. Naderi, M. Chapter Fourteen-Surface Area: Brunauer-Emmett-Teller (BET). In *Progress in Filtration and Separation*; Academic Press: Cambridge, MA, USA, 2015; pp. 585–608.
23. Romero-Cano, L.A.; González-Gutiérrez, L.V.; Baldenegro-Pérez, L.A.; Medina-Montes, M.I. Preparation of orange peles by instant controlled pressure drop and chemical modification for its use as biosorbent of organic pollutants. *Revista Mexicana Ingeniería Química* **2016**, *15*, 481–491.
24. Zhang, C.; Zhang, Z.; Zhang, L.; Li, Q.; Li, C.; Chen, G.; Zhang, S.; Liu, Q.; Hu, X. Evolution of the functionalities and structures of biochar in pyrolysis of poplar in a wide temperature range. *Bioresour. Technol.* **2020**, *304*, 123002. [CrossRef] [PubMed]
25. Sánchez, F.; Araus, K.; Domínguez, M.P.; San Miguel, G. Thermochemical Transformation of Residual Avocado Seeds: Torrefaction and Carbonization. *Waste Biomass Valoriz.* **2017**, *8*, 2495–2510. [CrossRef]
26. Alkurdi, S.S.; Al-Juboori, R.A.; Bundschuh, J.; Bowtell, L.; McKnight, S. Effect of pyrolysis conditions on bone char characterization and its ability for arsenic and fluoride removal. *Environ. Pollut.* **2020**, *262*, 114221. [CrossRef]
27. Menya, E.; Olupot, P.W.; Storz, H.; Lubwama, M.; Kiros, Y.; John, M.J. Optimization of pyrolysis conditions for char production from rice husks and its characterization as a precursor for production of activated carbon. *Biomass Convers. Biorefin.* **2019**, *10*, 57–72. [CrossRef]
28. Shakya, A.; Agarwal, T. Removal of Cr(VI) from water using pineapple peel derived biochars: Adsorption potential and re-usability assessment. *J. Mol. Liq.* **2019**, *293*, 111497. [CrossRef]
29. Guerrero, M.; Ruiz, M.P.; Millera, A.; Alzueta, M.; Bilbao, R. Characterization of Biomass Chars Formed under Different Devolatilization Conditions: Differences between Rice Husk and Eucalyptus. *Energy Fuels* **2008**, *22*, 1275–1284. [CrossRef]
30. Ji, B.; Zhu, L.; Song, H.; Chen, W.; Guo, S.; Chen, F. Adsorption of Methylene Blue onto Novel Biochars Prepared from Magnolia grandiflora Linn Fallen Leaves at Three Pyrolysis Temperatures. *Water Air Soil Pollut.* **2019**, *230*, 281. [CrossRef]
31. Vafajoo, L.; Cheraghi, R.; Dabbagh, R.; McKay, G. Removal of cobalt (II) ions from aqueous solutions utilizing the pre-treated 2-Hypnea Valentiae algae: Equilibrium, thermodynamic, and dynamic studies. *Chem. Eng. J.* **2018**, *331*, 39–47. [CrossRef]
32. Angın, D.; Şensöz, S. Effect of Pyrolysis Temperature on Chemical and Surface Properties of Biochar of Rapeseed (*Brassica napus* L.). *Int. J. Phytoremediation* **2014**, *16*, 684–693. [CrossRef]
33. Patel, S.; Han, J.; Qiu, W.; Gao, W. Synthesis and characterisation of mesoporous bone char obtained by pyrolysis of animal bones, for environmental application. *J. Environ. Chem. Eng.* **2015**, *3*, 2368–2377. [CrossRef]
34. Zhang, P.; Zheng, S.; Liu, J.; Wang, B.; Liu, F.; Feng, Y. Surface properties of activated sludge-derived biochar determine the facilitating effects on Geobacter co-cultures. *Water Res.* **2018**, *142*, 441–451. [CrossRef]
35. King, P.; Rakesh, N.; Beenalahari, S.; Prasanna Kumar, Y.; Prasad, V.S.R.K. Removal of lead from aqueous solution using *Syzygium cumini* L.: Equilibrium and kinetic studies. *J. Hazard. Mater.* **2007**, *142*, 340–347. [CrossRef] [PubMed]

36. Da Silva, D.C.C.; Pietrobelli, J.M.T.D.A. Residual biomass of chia seeds (*Salvia hispanica*) oil extraction as low cost and eco-friendly biosorbent for effective reactive yellow B2R textile dye removal: Characterization, kinetic, thermodynamic and isotherm studies. *J. Environ. Chem. Eng.* **2019**, *7*, 103008. [CrossRef]
37. Kostas, K.; Dimitra, Z.; Ioannis, P.; Despina, V.; Georgios, B. Assessment of pistachio shell biochar quality and its potential for adsorption of heavy metals. *Waste Biomass Valoriz.* **2015**, *6*, 805–816.
38. Lagergren, S.K. About the theory of so-called adsorption of soluble substances. *Sven. Vetenskapsakad. Handl.* **1898**, *24*, 1–39.
39. Ho, Y.S.; McKay, G. Sorption of dye from aqueous solution by peat. *Chem. Eng. J.* **1998**, *70*, 115–124. [CrossRef]
40. Liu, J.; Huang, Z.; Chen, Z.; Sun, J.; Gao, Y.; Wu, E. Resource utilization of swine sludge to prepare modified biochar adsorbent for the efficient removal of Pb(II) from water. *J. Clean. Prod.* **2020**, *257*, 120332. [CrossRef]
41. Saletnik, B.; Zagula, G.; Grabek-Lejko, D.; Kasprzyk, I.; Bajcar, M.; Czernicka, M.; Puchalski, C. Biosorption of cadmium (II), lead (II) and cobalt (II) from aqueous solution by biochar from cones of larch (*Larix decidua* Mill. Subsp. *Decidua*) and spruce (*Picea abies* L. H. Karst). *Environ. Earth Sci.* **2017**, *76*, 574.
42. Langmuir, I. The adsorption of gases on plane surfaces of glass, mica and platinum. *J. Am. Chem. Soc.* **1918**, *40*, 1361–1403. [CrossRef]
43. Freundlich, H. *Colloid and Capillary Chemistry*; Methuen: London, UK, 1926.
44. Farnane, M.; Tounsadi, H.; Elmoubarki, R.; Mahjoubi, F.; Elhalil, A.; Saqrane, S.; Abdennouri, M.; Qourzal, S.; Barka, N. Alkaline treated carob shells as sustainable biosorbent for clean recovery of heavy metals: Kinetics, equilibrium, ions interference and process optimisation. *Ecol. Eng.* **2017**, *101*, 9–20. [CrossRef]
45. Parab, H.; Joshi, S.; Shenoy, N.; Lali, A.; Sarma, U.; Sudersanan, M. Determination of kinetic and equilibrium parameters of the batch adsorption of Co(II), Cr(III) and Ni(II) onto coir pith. *Process. Biochem.* **2006**, *41*, 609–615. [CrossRef]
46. Tounsadi, H.; Khalidi, A.; Abdennouri, M.; Barka, N. Biosorption potential of Diplotaxis harra and *Glebionis coronaria* L. biomasses for the removal of Cd(II) and Co(II) from aqueous solutions. *J. Environ. Chem. Eng.* **2015**, *3*, 822–830. [CrossRef]
47. Bhatnagar, A.; Minocha, A.; Sillanpää, M. Adsorptive removal of cobalt from aqueous solution by utilizing lemon peel as biosorbent. *Biochem. Eng. J.* **2010**, *48*, 181–186. [CrossRef]
48. Vijayaraghavan, K.; Jegan, J.; Palanivelu, K.; Velan, M. Biosorption of cobalt(II) and nickel(II) by seaweeds: Batch and column studies. *Sep. Purif. Technol.* **2005**, *44*, 53–59. [CrossRef]
49. Tofan, L.; Teodosiu, C.; Păduraru, C.; Wenkert, R. Cobalt (II) removal from aqueous solutions by natural hemp fibers: Batch and fixed-bed column studies. *Appl. Surf. Sci.* **2013**, *285*, 33–39. [CrossRef]
50. Güzel, F.; Yakut, H.; Topal, G. Determination of kinetic and equilibrium parameters of the bath adsorption of Mn(II), Co(II), Ni(II) and Cu(II) from aqueous solution by black carrot (*Daucus carota* L.) residues. *J. Hazard. Mater.* **2008**, *153*, 1275–1287. [CrossRef]
51. Ibrahim, W.M. Biosorption of heavy metal ions from aqueous solution by red macroalgae. *J. Hazard. Mater.* **2011**, *192*, 1827–1835. [CrossRef]
52. Javed, M.A.; Bhatti, H.N.; Hanifa, M.A.; Nadeem, R. Kinetic and Equilibrium Modeling of Pb(II) and Co(II) Sorption onto Rose Waste Biomass. *Sep. Sci. Technol.* **2007**, *42*, 3641–3656. [CrossRef]
53. Oguz, E.; Ersoy, M. Biosorption of cobalt(II) with sunflower biomass from aqueous solutions in a fixed bed column and neural networks modelling. *Ecotoxicol. Environ. Saf.* **2014**, *99*, 54–60. [CrossRef]
54. Demirbaş, E. Adsorption of Cobalt(II) Ions from Aqueous Solution onto Activated Carbon Prepared from Hazelnut Shells. *Adsorpt. Sci. Technol.* **2003**, *21*, 951–963. [CrossRef]

© 2020 by the authors. Licensee MDPI, Basel, Switzerland. This article is an open access article distributed under the terms and conditions of the Creative Commons Attribution (CC BY) license (http://creativecommons.org/licenses/by/4.0/).